# Sieving of nanometer Enantiomers using Bound states in the continuum from Metasurface

*Libang Mao[a,b], Peiyuan Cheng[a], Kuan Liu[a], Meng Lian[a], and Tun Cao[a,b,*],*

[a]School of Optoelectronic Engineering and Instrumentation Science, Dalian University of Technology, Dalian 116024, China

[b]These authors contributed equally: Tun Cao, Libang Mao.

KEYWORDS: bound states, dielectric metasurface, enantioseparation, chiral nanoparticle

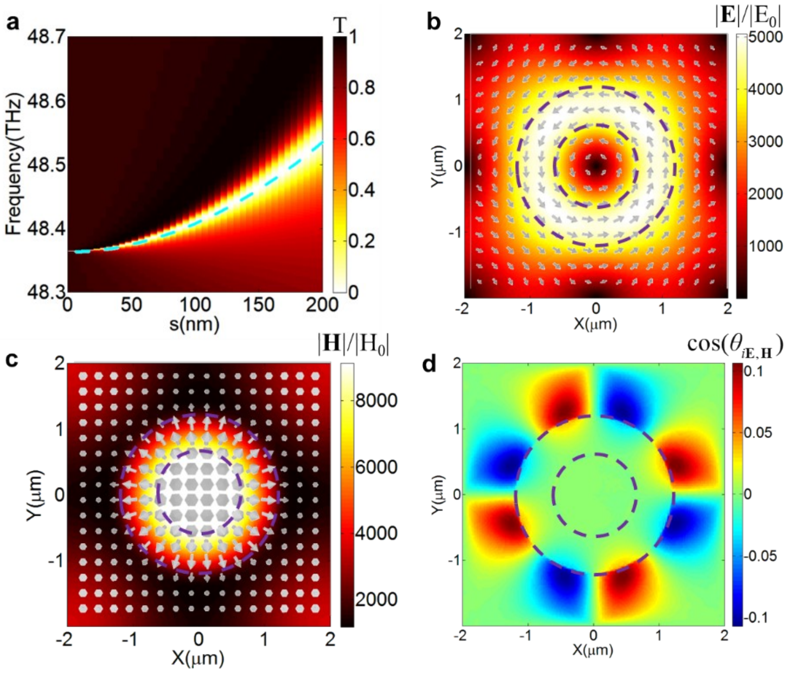


**Figure** S1. (a) The transmittance spectra and eigenmode spectra against the offset of a hole ($s$) for Si disk-hole metasurface. The cyan dashed line demonstrates the dispersion of eigenmode. Distributions of (b) E-field enhancement $|\mathbf{E}|/|E_0|$, (c) H-field enhancement $|\mathbf{H}|/|H_0|$, and (d) cos ($\theta_{i\mathbf{E},\ \mathbf{H}}$) at the quasi-BIC MD resonance ( $\lambda$ = 6203 nm), where the gray arrow represents the vector of E- and H-field.

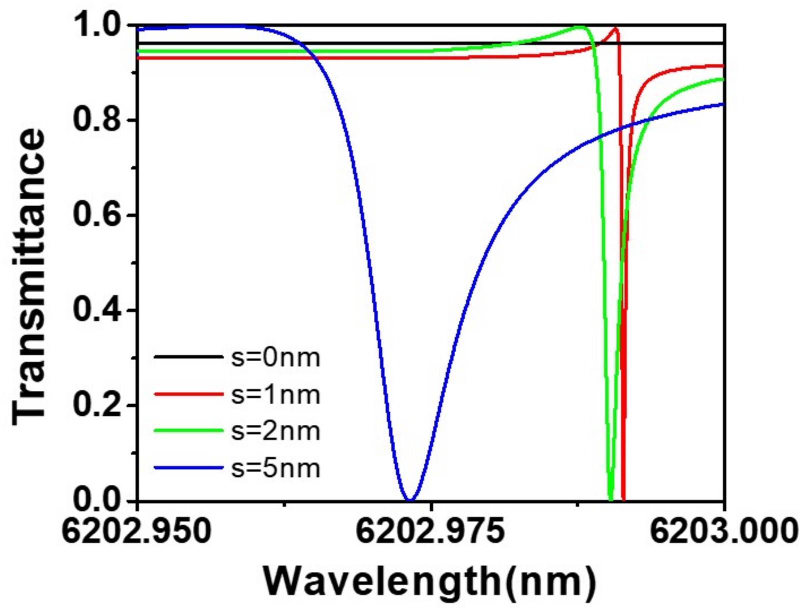


**Figure** S2. The simulated transmittance spectra through the metasurfaces with $s$= 0, 1, 2, and 5 nm under linearly polarised (LP) incidence.

A chiral particle whose dimensions are significantly smaller than the spatial change of the surrounding harmonic EM field can be described as a pair of interacting electric $\mathrm{P} = \mathrm{Re}[\mathbf{p}(\mathbf{r})\mathbf{e}^{-\mathrm{i}\omega t}]$ and magnetic $\mathbf{M} = \mathrm{Re}[\mathbf{m}(\mathbf{r})\mathbf{e}^{-\mathrm{i}\omega t}]$ dipolar moments, in which the chiral particle subjected to the monochromatic EM-field generates the moments of $\mathbf{p}$ and $\mathbf{m}$ associate with both the local electric $\mathbf{E}$ and magnetic $\mathbf{H}$ fields at the particle that are expressed as[1]

$$\begin{pmatrix} \mathbf{p} \\ \mathbf{m} \end{pmatrix} = \begin{pmatrix} \alpha\varepsilon_{\mathrm{s}} & i\chi\sqrt{\varepsilon_{\mathrm{s}}\mu_{\mathrm{s}}} \\ -i\chi\sqrt{\varepsilon_{\mathrm{s}}\mu_{\mathrm{s}}} & \beta\mu_{\mathrm{s}} \end{pmatrix} \times \begin{pmatrix} \mathbf{E} \\ \mathbf{H} \end{pmatrix} \tag{S1}$$

where the $\varepsilon_{\mathrm{s}}$ and $\mu_{\mathrm{s}}$ are the permittivity and permeability of the surrounding media; the electric $\alpha$, magnetic $\beta$ and mixed electric-magnetic $\chi$ dipole polarizabilities are complex scalars. Particularly, the sign (+, -) of $\chi$ polarisability is closely related to the handedness of enantiomers associated with the dipolar system in Eq. (S1). Noteworthy, the $\alpha$ and $\beta$ polarizabilities are always the same during enantiomeric variations as they are quadratic forms of the electric and magnetic dipoles accordingly. Therefore, one of our purposes is to discriminate the effect of the sign change of $\chi$ on optical forces exerted on chiral dipoles.

For a nanosphere, the polarisabilities of $\alpha$, $\beta$ and $\chi$ can be simply shown as[2]:

$$\alpha = 4\pi r_{\mathbf{p}}^{3} \frac{(\varepsilon_{\mathbf{r}}-1)(\mu_{\mathbf{r}}+2)-\kappa_{\mathbf{p}}^{2}}{(\varepsilon_{\mathbf{r}}+2)(\mu_{\mathbf{r}}+2)-\kappa_{\mathbf{p}}^{2}} \tag{S2}$$

$$\beta = 4\pi r_{\mathbf{p}}^{3} \frac{(\mu_{\mathbf{r}}-1)(\varepsilon_{\mathbf{r}}+2)-\kappa_{\mathbf{p}}^{2}}{(\varepsilon_{\mathbf{r}}+2)(\mu_{\mathbf{r}}+2)-\kappa_{\mathbf{p}}^{2}} \tag{S3}$$

$$\chi = 12\pi r_{\mathbf{p}}^{3} \frac{\kappa_{\mathbf{p}}}{(\varepsilon_{\mathbf{r}}+2)(\mu_{\mathbf{r}}+2)-\kappa_{\mathbf{p}}^{2}} \tag{S4}$$

$\varepsilon_{\mathrm{r}}=\varepsilon_{\mathrm{p}}/\varepsilon_{\mathrm{s}}$, $\mu_{\mathrm{r}}=\mu_{\mathrm{p}}/\mu_{\mathrm{s}}$ are the relative permittivity and permeability, with respect to the surrounding media; ($\varepsilon_{\mathrm{p}}$, $\mu_{\mathrm{p}}$) gives the refractive index $n_{\mathrm{p}}$ of the nanosphere; and $\varepsilon_{\mathrm{s}}$ and $\mu_{\mathrm{s}}$ are the dielectric permittivity and magnetic permeability of the surrounding medium. $\kappa_{\mathrm{p}}$ determines the chirality of the sphere that links to the effective refractive index difference $n_{\pm} = n_{\mathrm{s}} \pm \kappa_{\mathrm{p}}$ between left (-) and right (+) handed circularly polarized waves, and it measures the level of handedenss of chiral molecules. Thus, the imaginary part of $\kappa_{\mathrm{p}}$ ($\mathrm{Im}(\kappa_{\mathrm{p}})$) is related to the chiral response and the real part ($\mathrm{Re}(\kappa_{\mathrm{p}})$) to the optical rotation. $r_{\mathrm{p}}$ is the radius of nanoparticle. The time-averaged optical force $\mathbf{F}_{\mathbf{t}}$ exerted on a chiral particle can be expressed from the Lorentz force law[1, 3]:

$$\mathbf{F}_{\mathrm{t}} = \frac{1}{2}\mathrm{Re}\left[(\mathbf{p}\cdot\nabla)\mathbf{E}^{*} + (\mathbf{m}\cdot\nabla)\mathbf{H}^{*} - i\omega\mu_{\mathrm{s}}\mathbf{p}\times\mathbf{H}^{*} + i\omega\varepsilon_{\mathrm{s}}\mathbf{m}\times\mathbf{E}^{*}\right] \tag{S5}$$

Note that, herein we do not take account of the terms stemming from self-interactions of the dipole that plays the role in producing the recoil force. The $\mathbf{F}_{\mathrm{t}}$ can then be presented as a sum of a non-chiral gradient force ($\mathbf{F}_{\alpha,\beta}$) and chiral gradient force ($\mathbf{F}_{\chi}$), associated with ($\alpha$, $\beta$) and $\chi$ polarizabilities accordingly.

$$\mathbf{F}_{\mathbf{t}} = \mathbf{F}_{\alpha,\beta} + \mathbf{F}_{\chi} \tag{S6}$$

By placing the dipolar moments ($\mathbf{p}$, $\mathbf{m}$) shown in Eq. (S1) into Eq. (S5), the $\mathbf{F}_{\alpha,\beta}$ and $\mathbf{F}_{\chi}$ can be both divided into reactive and dissipative constituents, which consists of the real and imaginary parts of the $\alpha$, $\beta$ and $\chi$ polarisabilities:

$$\mathbf{F}_{\chi}^{\text{reac}} = -\frac{c^2}{\omega}\text{Re}\left[\chi\right]\cdot\nabla C \tag{S7}$$

$$\mathbf{F}_{\chi}^{\text{diss}} = \frac{2}{c}\sqrt{\frac{\varepsilon_{\mathbf{s}}\mu_{\mathbf{s}}}{\varepsilon_0\mu_0}}\,\text{Im}\left[\chi\right]\cdot\left(\Phi - \frac{\nabla\times\Pi}{2}\right) \tag{S8}$$

$$\mathbf{F}_{\alpha,\beta}^{\text{reac}} = \text{Re}\left[\alpha\right]\nabla W_{\text{E}} + \text{Re}\left[\beta\right]\nabla W_{\text{H}} \tag{S9}$$

$$\mathbf{F}_{\alpha,\beta}^{\text{diss}} = \frac{\omega\varepsilon_{\mathbf{s}}\mu_{\mathbf{s}}}{c^2\varepsilon_0\mu_0}(\text{Im}\left[\alpha\right]\mathbf{\Pi}_{\text{O}}^{(\text{E})} + \text{Im}\left[\beta\right]\mathbf{\Pi}_{\text{O}}^{(\text{H})}) \tag{S10}$$

where $W_{\text{E}} = \frac{\varepsilon_{\text{s}}}{4}\left\|\mathbf{E}\right\|^2$ and $W_{\text{H}} = \frac{\mu_{\text{s}}}{4}\left\|\mathbf{H}\right\|^2$ are the energy densities of both E and H field respectively, $\Pi_{\text{O}}^{(\text{E})} = \Pi - \frac{\nabla\times\Phi_{\text{E}}}{2\omega\mu_{\text{s}}}$ and $\Pi_{\text{O}}^{(\text{H})} = \Pi - \frac{\nabla\times\Phi_{\text{H}}}{2\omega\varepsilon_{\text{s}}}$ are for both electric and magnetic orbital parts of the Poynting vector $\Pi = \frac{\text{Re}\left[\mathbf{E}\times\mathbf{H}^*\right]}{2}$ accordingly, $C = -\frac{\omega}{2c^2}\text{Im}\left(\mathbf{E}^*\cdot\mathbf{H}\right)$ is the chirality density of the field and $\Phi$ is the flow of chirality. The flow of the chirality is determined by the E and H field ellipticities:

$$\Phi = \frac{\omega\left(\varepsilon_{\text{s}}\Phi_{\text{E}} + \mu_{\text{s}}\Phi_{\text{H}}\right)}{2} \tag{S11}$$

where $\Phi_{\text{E}} = -\frac{1}{2}\text{Im}\left[\mathbf{E}\times\mathbf{E}^*\right]$ and $\Phi_{\text{H}} = -\frac{1}{2}\text{Im}\left[\mathbf{H}\times\mathbf{H}^*\right]$.

As can be seen in Eq. (S6), the variation between the total gradient force $\mathbf{F}_{\mathbf{t}}$ of a paired enantiomers originates from the addition or subtraction between the non-chiral gradient force $\mathbf{F}_{\alpha,\beta}$ and chiral gradient force $\mathbf{F}_{\chi}$, where $\mathbf{F}_{\chi}$ is directly related to the optical chirality density of the field. Note that, the $\mathbf{F}_{\chi}$ is mainly controlled by $\mathbf{F}_{\chi}^{\text{reac}}$ , since $\mathbf{F}_{\chi}^{\textbf{diss}}$ which is associated with Im[ $\chi$ ], can be ignored due to the small imaginary part of the particle's permittivity (Im (ε) = 0). As can be seen in $\mathbf{F}_{\chi}^{\text{reac}}$, two chiral entities possessing the different $\chi$ experience $\mathbf{F}_{\chi}$ in the opposite directions, and the achievement of a giant $\nabla C$ is important to obtain a large $\mathbf{F}_{\chi}$. **Figure** S3(a) presents the $\nabla C$ for the quasi-BIC resonant mode (λ= 6203 nm) ; the color represent the strength of $\nabla C$. This indicates that the quasi-BIC mode leads to the strongest $\nabla C$ around the outer edge of the Si disk, enabling a strong $\mathbf{F}_{\chi}$ on the chiral entities. In the contrary, one needs to reduce the $\mathbf{F}_{\alpha,\beta}$ to make it much smaller than the $\mathbf{F}_{\chi}$ thus obtaining an efficient enantioseparation. $\mathbf{F}_{\alpha,\beta}$ is composed by two time-averaged achiral gradient forces offered by the reactive force $\mathbf{F}_{\alpha,\beta}^{\text{reac}}$ and dissipative force $\mathbf{F}_{\alpha,\beta}^{\text{diss}}$. The $\mathbf{F}_{\alpha,\beta}^{\text{diss}}$ appears to be zero owing to the ultrasmall Im(ε)=0. Therefore, the $\mathbf{F}_{\alpha,\beta}$ is dominated by the $\mathbf{F}_{\alpha,\beta}^{\text{reac}}$ relating to both magnetic ($\nabla W_{\mathbf{H}}$) and electric ($\nabla W_{\mathrm{E}}$) energy densities. **Figure** S3b-S3c present $\nabla W_{\mathrm{E}}$ and $\nabla W_{\mathbf{H}}$ at quasi-BIC resonant mode (λ= 6203 nm). Noted that the maximum in both $\nabla W_{\mathrm{E}}$ and $\nabla W_{\mathbf{H}}$ don not overlap with the largest $\nabla C$ and the quasi-BIC resonance can improve the $\nabla C$ more significant than $\nabla W_{\mathrm{E}}$ and $\nabla W_{\mathbf{H}}$ thus offer a much stronger $\mathbf{F}_{\chi}$ to conquer $\mathbf{F}_{\alpha,\beta}$. Therefore, $\mathbf{F}_{\mathbf{t}}$ can be controlled by $\mathbf{F}_{\chi}$, which separates the chiral entities with opposite handednesses.

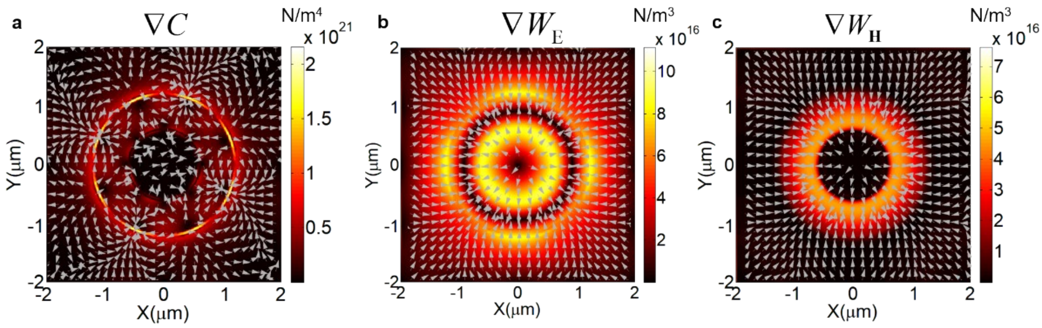


**Figure S3.** Distributions of (a) chirality density gradient $\nabla C$, (b) electric energy density $\nabla W_{\mathrm{E}}$, and (c) magnetic energy density $\nabla W_{\mathbf{H}}$ in quasi-BICs resonance mode (at λ= 6203 nm) .

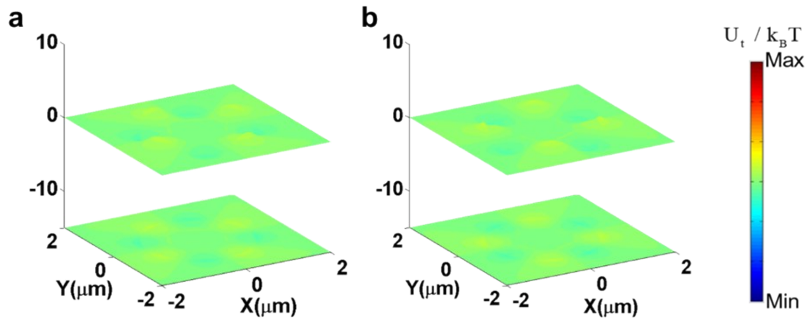

**Figure S4.** Surface potential ($U_t$) under an illumination of linearly polarised light for the (a) LH- ($\kappa_p$ = -0.001) and (b) RH- ($\kappa_p$ = +0.001) enantiomers with $r_p$ = 2 nm at 20 nm above the surface of the quasi-BIC MD meta-atom with $s$ = 1 nm at λ= 6203 nm .

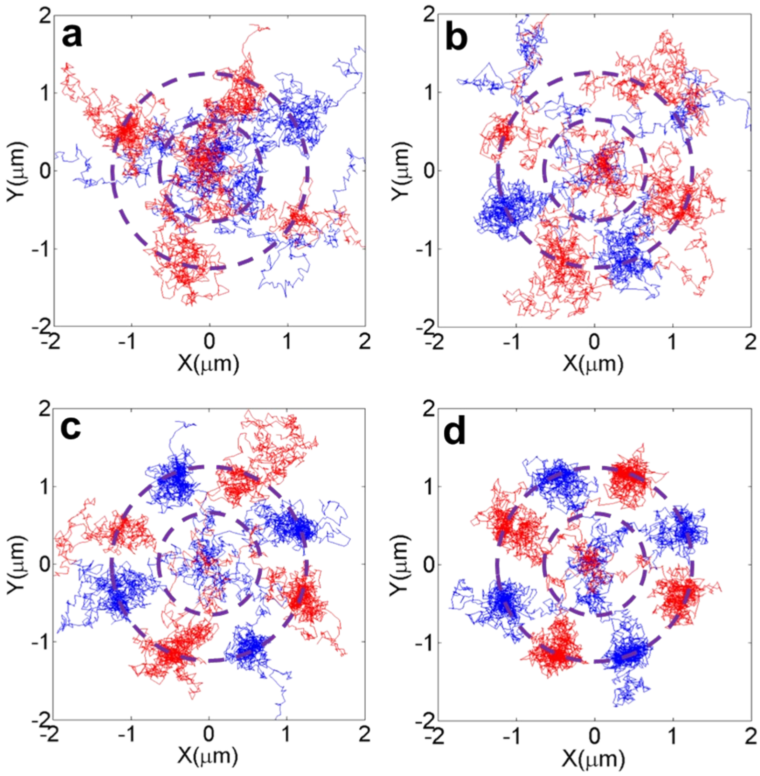


**Figure S5.** The stability of the enantiomeric pair ($r_p$ =2 nm, $\kappa_p$ = ±0.001) under the different illumination intensities ($I_{in}$), where the red and blue solid lines represent the 10 ms trajectories of the LH- and RH- enantiomers, respectively, (a) $I_{in}$ = 200 mW/μm$^2$ (b) $I_{in}$ = 300 mW/μm$^2$, (c) $I_{in}$ = 400 mW/μm$^2$, (d) $I_{in}$ = 500 mW/μm$^2$.

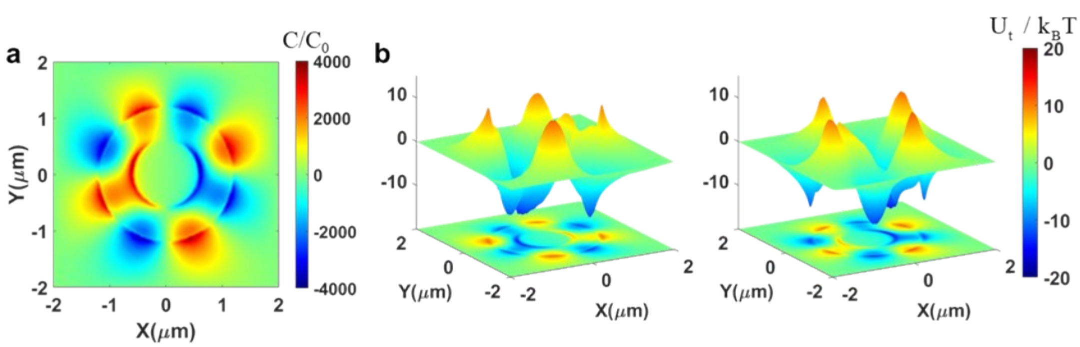


**Figure S6.** (a) The distributions of $C/C_0$ in the resonator with the off-sets of $s$ = 20 nm. (b) Surface potential ($U_t$) under an illumination of linearly polarised light for the LH- ($\kappa_p$ = -0.01) (left column) and the RH- ($\kappa_p$ = +0.01) (right column) enantiomers with $r_p$ = 14 nm at 20 nm above the surface of the quasi-BIC MD meta-atom with $s$ = 20 nm

**Supplementary References**


1. Canaguier-Durand, A.; Genet, C., Chiral route to pulling optical forces and left-handed optical torques. *Phys. Rev. A* **2015,** *92* (4), 043823.
2. Canaguier-Durand, A.; Genet, C., Plasmonic lateral forces on chiral spheres. *Journal of Optics* **2015,** *18* (1), 015007.
3. Canaguier-Durand, A.; Hutchison, J. A.; Genet, C.; Ebbesen, T. W., Mechanical separation of chiral dipoles by chiral light. *New Journal of Physics* **2013,** *15* (12), 123037.